

Article

Applied Thermodynamics: Grain Boundary Segregation

Pavel Lejček^{1,*}, Lei Zheng², Siegfried Hofmann³ and Mojmír Šob^{4,5,6}

- ¹ Laboratory of Nanostructures and Nanomaterials, Institute of Physics, Academy of Sciences of the Czech Republic (AS CR), Na Slovance 2, 182 21 Praha 8, Czech Republic; E-Mail: lejcekp@fzu.cz
- ² School of Materials Science and Engineering, University of Science and Technology Beijing, Beijing 100083, China; E-Mail: zhenglei ustb@sina.com
- ³ Max-Planck-Institute for Intelligent Systems, Heisenbergstr. 7, 70499 Stuttgart, Germany; E-Mail: hofmann@is.mpg.de
- ⁴ Central European Institute of Technology, CEITEC MU, Masaryk University, Kamenice 5, 625 00 Brno, Czech Republic
- ⁵ Institute of Physics of Materials, AS CR, Žižkova 22, 616 62 Brno, Czech Republic; E-Mail: mojmir@ipm.cz
- ⁶ Department of Chemistry, Faculty of Science, Masaryk University, Kotlářská 2, 611 37 Brno, Czech Republic; E-Mail: sob@chemi.muni.cz
- * Author to whom correspondence should be addressed; E-Mail: lejcekp@fzu.cz; Tel.: +420-266-052-167; Fax: +420-286-890-527.

Received: 5 February 2014; in revised form: 20 February 2014 / Accepted: 28 February 2014 / Published: 12 March 2014

Abstract: Chemical composition of interfaces—free surfaces and grain boundaries—is generally described by the Langmuir–McLean segregation isotherm controlled by Gibbs energy of segregation. Various components of the Gibbs energy of segregation, the standard and the excess ones as well as other thermodynamic state functions—enthalpy, entropy and volume—of interfacial segregation are derived and their physical meaning is elucidated. The importance of the thermodynamic state functions of grain boundary segregation, their dependence on volume solid solubility, mutual solute–solute interaction and pressure effect in ferrous alloys is demonstrated.

Keywords: interfacial segregation; Gibbs energy of segregation; enthalpy; entropy; volume; grain boundaries; iron

PACS Codes: 68.35.bd; 68.35.Dv; 68.35.Md; 65.40.gd; 82.65.+r;

1. Introduction

The fundamental laws of thermodynamics are applied in many fields of materials science. Their application is particularly important in the field of *interfacial segregation*, *i.e.* the accumulation of solute or impurity atoms at an interface. The segregation results in changing bonds at the interface and—in the case of grain boundaries (i.e. interfaces between two differently oriented crystals in a solid)-often in their weakening which results in reduction of material cohesion and consequently, in intergranular brittle fracture leading to irreversible degradation of the material [1]. Although numerous papers published in the last decades provide us with a database of chemical composition of interfaces under specific conditions (for reviews see e.g. [2,3]), it is more desirable to disclose general trends that are capable of predicting materials' behavior under different thermal and structural conditions using appropriate thermodynamic variables [4,5]. Unfortunately, some thermodynamic data published in literature are of unclear physical meaning and their incorrect interpretation can result in misunderstanding of the fundamentals of interfacial segregation. To avoid this problem, we characterize individual components of the Gibbs energy of grain boundary segregation and consequently, their enthalpy, entropy and volume counterparts, and show the differences among them. Additionally, a reliable application of the basic thermodynamic state functions—the standard enthalpy and entropy of interfacial segregation-as well as of the excess volume is shown.

2. Langmuir–McLean Segregation Isotherm

Of the two different approaches describing interfacial segregation in a general way, *i.e.* the *Gibbs* segregation isotherm and the *Langmuir–McLean* segregation isotherm, the latter is more convenient (and thus applied as well) as it operates with characteristic changes of the Gibbs energy, *G* (e.g. [1,4,5]). In this approach the segregation of a solute *I* at an interface Φ in a binary *M–I* system can be understood as an exchange of the components *M* and *I* between Φ and the volume *V* [6]:

$$M^{\Phi} + I^{V} \Leftrightarrow M^{V} + I^{\Phi} \tag{1}$$

The molar Gibbs energy of "reaction" (1), ΔG_r , being the difference of the chemical potentials, μ_j^{ζ} (let us note that index *j* denotes any component in the system throughout the whole paper, *i.e. j* = *I*,*M* here, and $\zeta = \Phi$,*V*), of the right-hand and left-hand terms, is equal to zero in equilibrium [6]:

$$\Delta G_r = \left(\mu_{I(M)}^{\Phi} + \mu_M^V\right) - \left(\mu_{I(M)}^V + \mu_M^{\Phi}\right) = 0$$
⁽²⁾

In Equation (2), $\mu_j^{\zeta} = \mu_{j(M)}^{\zeta,0} + RT \ln a_j^{\zeta}$, where $\mu_{j(M)}^{\zeta,0}$ is the standard chemical potential of pure component *j* at temperature *T* and structure of *M* (for *j* = *M*, we use simple notation "*M*" instead of the notation *M*(*M*)), and a_j^{ζ} is the activity of *j* at ζ . As this definition is applicable to both the crystal volume *V* and the interface Φ , we obtain:

$$\frac{a_I^{\Phi}}{a_M^{\Phi}} = \frac{a_I^V}{a_M^V} \exp\left(-\frac{\Delta G_I^0}{RT}\right)$$
(3)

with the standard molar Gibbs energy of segregation:

$$\Delta G_{I}^{0} = \left(\mu_{I(M)}^{\Phi,0} + \mu_{M}^{V,0}\right) - \left(\mu_{I(M)}^{V,0} + \mu_{M}^{\Phi,0}\right)$$
(4)

The activities in Equation (3) can be replaced by concentrations, $a_j^{\zeta} = \gamma_j^{\zeta} X_j^{\zeta}$, where γ_j^{ζ} are the activity coefficients, and X_j^{ζ} are the atomic fractions of components *j* for $\zeta = \Phi$, *V*. Consequently:

$$\frac{X_I^{\Phi}}{1 - X_I^{\Phi}} = \frac{X_I^V}{1 - X_I^V} \exp\left(-\frac{\Delta G_I}{RT}\right) = \frac{X_I^V}{1 - X_I^V} \frac{\gamma_I^V \gamma_M^{\Phi}}{\gamma_M^V \gamma_I^{\Phi}} \exp\left(-\frac{\Delta G_I^0}{RT}\right) = \frac{X_I^V}{1 - X_I^V} \exp\left(-\frac{\Delta G_I^0 + \Delta \overline{G}_I^E}{RT}\right)$$
(5)

in a binary *M*–*I* system, accepting $X_M^{\zeta} = 1 - X_I^{\zeta}$ for both, the volume and the interface. In a multicomponent systems with limited amount of segregation sites, *i.e.* fraction of interface saturation $X^{\Phi,sat}$ [2], we may write Equation (5) as:

$$\frac{X_I^{\Phi}}{X^{\Phi,sat} - \sum_{j \neq M} X_j^{\Phi}} = \frac{X_I^V}{1 - \sum_{j \neq M} X_j^V} \exp\left(-\frac{\Delta G_I}{RT}\right)$$
(5a)

In Equations (5) and (5a), ΔG_I is the Gibbs energy of segregation consisting of two terms, ΔG_I^0 and $\Delta \overline{G}_I^E$ [1]:

$$\Delta G_I = \Delta G_I^0 + \Delta \overline{G}_I^E \tag{6}$$

where $\Delta \overline{G}_{I}^{E}$ is the partial molar *excess* Gibbs energy of segregation [1]:

$$\Delta \overline{G}_{I}^{E} = RT \ln \frac{\gamma_{I}^{\Phi} \gamma_{M}^{V}}{\gamma_{I}^{V} \gamma_{M}^{\Phi}}$$
⁽⁷⁾

Equation (5a) with condition (6) represents the general form of the segregation isotherm. It was derived without any non-thermodynamic assumption and, therefore, can be used to describe interfacial segregation independently of the system nature. However, a serious terminological misunderstanding exists as ΔG_I in Equations (5) and (5a) is frequently incorrectly called "excess Gibbs energy of segregation", ΔG^{xs} (e.g. [7]) or ΔG^{ex} (e.g. [8]). This ambiguous terminology thus evokes confusion. However, the meaning of *excess* in the sense of the Lewis theory of non-ideal solutions [9] is the only correct because it represents the deviations between real and ideal behavior (see Equation (6)). In fact, the adjective "interfacial excess" is an unnecessary over-determination because the term *interfacial* itself already denotes the extra contribution of interfaces with respect to the bulk, and therefore it should not be used in this context [5].

3. Thermodynamic State Functions in Interfacial Segregation and Their Physical Meaning

It is evident from the considerations above that there exist three types of thermodynamic state functions of interfacial segregation. In the case of the Gibbs energy, one speaks about the *Gibbs* energy of segregation, the standard (ideal) Gibbs energy of segregation and the excess Gibbs energy of segregation, the latter characterizing the difference between the Gibbs energy of segregation and the ideal Gibbs energy of segregation. In the following, we will explain the physical meaning of all relevant thermodynamic quantities including the segregation volume which is rarely treated in such a detail.

According to the basic thermodynamic definition:

$$G = H - TS \tag{8}$$

 ΔG_I^0 is composed of the standard molar enthalpy, ΔH_I^0 , and entropy, ΔS_I^0 , of segregation, both of which are defined in the same way as ΔG_I^0 in Equation (4), *i.e.*:

$$\Delta H_I^0 = \left(h_{I(M)}^{\Phi,0} + h_M^{V,0} \right) - \left(h_M^{\Phi,0} + h_I^{V,0} \right) \quad \text{and}$$
(9a)

$$\Delta S_I^0 = \left(s_{I(M)}^{\Phi,0} + s_M^{V,0} \right) - \left(s_M^{\Phi,0} + s_I^{V,0} \right)$$
(9b)

where $h_j^{\Phi,0}$ and $h_j^{V,0}$, and $s_j^{\Phi,0}$ and $s_j^{V,0}$ are the respective molar enthalpy and entropy parts of the chemical potentials of solute *j* at Φ and *V*. Let us mention that ΔS_I^0 involves all entropy contributions except the configuration entropy [1,5]. As the segregation data are frequently correlated according to the Guttmann model of interfacial segregation in multicomponent systems [10], in which only the summary term $\Delta \overline{G}_I^E$ (which contains all interaction terms) appears:

$$\Delta G_I = \Delta H_I - T \Delta S_I = \left(\Delta H_I^0 - T \Delta S_I^0 \right) + \Delta \overline{G}_I^E \tag{10}$$

where ΔH_I and ΔS_I are the molar enthalpy and molar entropy of segregation of I at interface Φ .

Application of the fundamental thermodynamic relationship to the grain boundary segregation provides us with [11]:

$$d\Delta G_I = -\Delta S_I dT + \Delta V_I dP + \sum_{j,\xi} \mu_j^{\zeta} dX_j^{\zeta} + \sigma dA$$
⁽¹¹⁾

where σ is the grain boundary energy and *A* is the grain boundary molar area. According to Equation (11) the *molar segregation volume*, ΔV_I , is defined as:

$$\Delta V_I = \left(\frac{\partial \Delta G_I}{\partial P}\right)_{T,A,X_I^{\zeta}} \tag{12}$$

 ΔV_I is constructed in the same way as other segregation quantities:

$$\Delta V_I = \left(V_I^{\Phi} + V_M^{V}\right) - \left(V_M^{\Phi} + V_I^{V}\right) \tag{13}$$

Equation (13) is very close to Equation (1) in Reference [12] for $\Phi = GB$ supposing the relaxations terms α and V_r [12] are inherently implemented in the four terms of Equation (13). In the following we will discuss the segregation volume for grain boundaries.

Similarly to ΔG_I (Equation (6)), ΔV_I also consists of two parts, the standard molar segregation volume, ΔV_I^0 , and the partial molar excess segregation volume, $\Delta \overline{V}_I^E$:

$$\Delta V_I = \Delta V_I^0 + \Delta \overline{V}_I^E \tag{14}$$

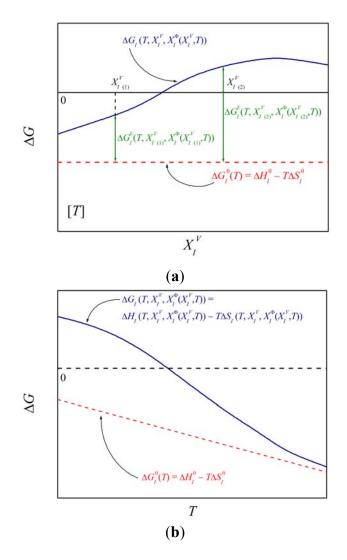
As ΔV_I is not involved in any model, we will treat this quantity separately later.

Let us note that in some cases the values of the thermodynamic variables are improperly interpreted, resulting in a lack of physical meaning. For example, this is the case when a single value of ΔG_I is determined on basis of the measurements of X_I^{Φ} at different temperatures (e.g., with Equation (5)) but averaged over the whole temperature range so that it represents an *effective* value. Similarly, an averaging may be done for systems with different bulk compositions or over numerous interfaces of different crystallography in polycrystals. For details see e.g. References [1,5].

3.1. Thermodynamic State Functions of Interfacial Segregation: ΔG_I , ΔH_I , ΔS_I and ΔV_I

Among the state functions of this mode, the Gibbs energy of interfacial segregation, ΔG_I , is the most important one as it completely determines interfacial concentration, X_I^{Φ} , at temperature *T* for bulk atomic fraction, X_I^V (*cf.* Equation (5a)). Its importance consists in reflecting the real behavior of the system as indicated by Equation (10). Principally, ΔG_I changes not only with changing temperature but also with changing concentrations X_I^V and X_I^{Φ} due to solute interaction (Figure 1). The corresponding values of ΔH_I and ΔS_I may also depend on temperature and concentration [1,5]. This means that these values can hardly provide us with any general information, e.g. about the anisotropy of grain boundary segregation, because any orientation dependence of ΔH_I and ΔS_I varies in a complex way with temperature and composition [1,5].

Figure 1. Schematic representation of the dependence of the types of ΔG_I^{ζ} (ΔG_I , ΔG_I° and $\Delta \overline{G}_I^E$) appearing in Equation (6) on (**a**) bulk concentration, and (**b**) temperature, both in a binary system [1].



Besides ΔG_I , ΔH_I and ΔS_I , the segregation volume, ΔV_I , may be considered as another variable of equal importance. However, it seems that it has not been included in the description of interfacial segregation till now.

It follows from Equations (5a) and (12), that in case of a binary system *M*–*I* [13]:

$$\Delta V_I = -\frac{RTX^{GB,sat}}{X_I^{GB}(X^{GB,sat} - X_I^{GB})} \frac{dX_I^{GB}}{dP}$$
(15)

Integration of Equation (15) results in an expression showing that the segregation volume plays an important role in grain boundary segregation under pressure:

$$\frac{X_{I}^{GB}(P)}{X^{GB,sat} - \sum_{j \neq M} X_{j}^{GB}(P)} = \frac{X_{I}^{GB}(P_{0})}{X^{GB,sat} - \sum_{j \neq M} X_{j}^{GB}(P_{0})} \exp\left[-\frac{(P - P_{0})\Delta V_{I}}{RT}\right]$$
(16)

where P_0 is the normal pressure. This relationship is principally similar to Equation (4) given by Zhang and Ren [14].

3.2. Standard Molar Thermodynamic Functions of Interfacial Segregation: ΔG_I^0 , ΔH_I^0 , ΔS_I^0 , $\Delta (c_P)_I^0$ and ΔV_I^0

The *standard molar* thermodynamic state functions possess a special importance in interfacial segregation as they have a very clear physical meaning. According to the definition (Equation (4)), ΔG_I^0 as a combination of standard chemical potentials, is principally *independent of concentration* (see Figure 1a). $\Delta G_I^0 = \Delta G_I$ only if $\Delta \overline{G}_I^E = 0$, *i.e.* if $\gamma_j^{\Phi} = \gamma_j^V = 1$ (Equations (5)–(7)). Certainly this represents a limitation although many systems behave nearly ideally (e.g. phosphorus in dilute Fe–P alloys [15,16]). Moreover, in an infinitesimally diluted solid solution the amount of interfacial solute enrichment is very low. Therefore it is highly probable that the solute atoms segregate at a those sites of the boundary which possess the lowest Gibbs segregation energy. Therefore, ΔG_I^0 *characterizes the interfacial segregation of element I at a specific site of interface* Φ *in the ideal system*. ΔH_I^0 and ΔS_I^0 are defined in analogy to ΔG_I^0 with corresponding physical meaning. According to Equations (3) and (8), the standard molar state functions control the relation between the activities at an interface and in the volume in the whole concentration range of a binary M–I system. Similarly to ΔG_I^0 and according to Equations (9a) and (9b), ΔH_I° and ΔS_I° are concentration independent. Analogously to ΔG_I^0 , ΔH_I^0 and ΔS_I^0 , we may define the standard molar specific heat of segregation, $\Delta (c_P)_I^{V,0}$, as a combination of molar specific heats of pure substances, $(c_P)_j^{\Phi,0}$ and $(c_P)_J^{V,0}$:

$$\Delta(c_P)_I^0 = \left((c_P)_{I(M)}^{\Phi,0} + (c_P)_M^{\Phi,0} \right) - \left((c_P)_{I(M)}^{V,0} + (c_P)_M^{V,0} \right) \equiv 0$$
(17)

The value $\Delta(c_p)_I^0 \equiv 0$ results from the fact that $(c_p)_j^{\zeta,0}$ are insensitive to the presence of structural defects such as dislocations as well as grain boundaries [17], *i.e.* although an increase of c_p was reported in case of nanocrystaline materials [18]. However, the different enhancements of c_p of nanocrystalline palladium and copper were ascribed to lower densities of these substances in the nanometer-sized crystalline state [18] representing transition between crystalline and glassy states. In case of a large bicrystal with specified grain boundary we may well accept the relation $(c_p)_{i(M)}^{\phi,0} = (c_p)_{i(M)}^{V,0}$. Then:

$$\left(\frac{\partial \Delta H_I^0}{\partial T}\right)_{P,X_i} = \Delta (c_P)_I^0 \equiv 0$$
(18a)

and

$$\left(\frac{\partial\Delta S_I^0}{\partial T}\right)_{P,X_i} = \frac{\Delta (c_P)_I^0}{T} \equiv 0$$
(18b)

It means that ΔH_I^0 and ΔS_I^0 are independent of temperature and ΔG_I^0 is thus a linear function of temperature. As the standard state is defined as pure component *j* at temperature *T* and *structure of M*, $V_{I(M)}^{GB,0} \equiv V_M^{GB,0}$ and $V_{I(M)}^{V,0} \equiv V_M^{V,0}$. Consequently, $\Delta V_I^0 = (V_{I(M)}^{GB,0} - V_{I(M)}^{V,0}) - (V_M^{GB,0} - V_M^{V,0}) \equiv 0$. It means that all non-zero contributions to ΔV_I originate from the real behavior of the system ($\Delta V_I = \Delta \overline{V_I}^E$). The fact that $\Delta V_I^0 = 0$ has a serious consequence for other standard state functions: According to Equation (12) and $(\partial \Delta S_I^0 / \partial P)_T = -(\partial \Delta V_I^0 / \partial T)_P$, both ΔG_I^0 and ΔS_I^0 , and consequently ΔH_I^0 are independent of pressure. The independence of temperature and pressure is a principal property of ΔH_I^0 and ΔS_I^0 which thus change exclusively with the structure (*i.e.* energy) of the interface (or an interface site) and with the nature of the system. Therefore, ΔH_I^0 and ΔS_I^0 can be used for general purposes, for example, to characterize the anisotropy of interfacial segregation which is directly related to the grain boundary classification [1,5] despite their application is limited to ideal (infinitesimally diluted) systems.

3.3. Excess Thermodynamic Functions of Interfacial Segregation: $\Delta \overline{G}_{I}^{E}$ and $\Delta \overline{V}_{I}^{E}$

According to Equation (6), the *excess molar* Gibbs energy of segregation, $\Delta \overline{G}_I^E$, represents the *difference between real and ideal behavior with respect to interfacial segregation* and is exactly defined by the a combination of the activity coefficients (Equation (7)). It is thus evident that $\Delta \overline{G}_I^E$ depends on composition and non-linearly on temperature (*cf.* schematic Figure 1b). However, the values of the activity coefficients are unknown and hardly measurable, particularly for interfaces. Therefore, $\Delta \overline{G}_I^E$ is usually approximated by various models, e.g. by the regular solid solution (Fowler) model for a binary system:

$$\Delta \overline{G}_{I}^{E} = -2\alpha_{IM} \frac{X_{I}^{\Phi}}{X^{0}}$$
⁽¹⁹⁾

where α_{IM} is the coefficient of binary *I*–*I* interaction in *M*, or by various models for segregation in multicomponent systems, e.g. by the Guttmann model:

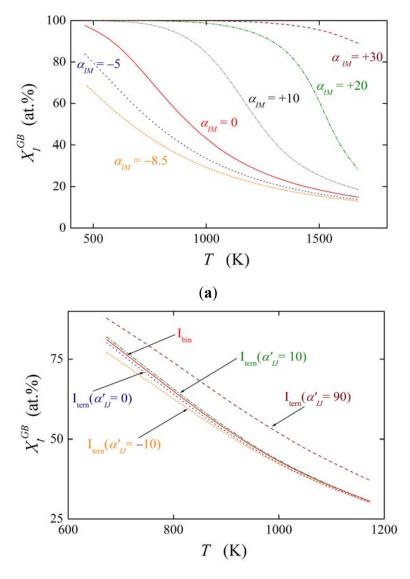
$$\Delta \overline{G}_I^E = -2\alpha_{IM}(X_I^\Phi - X_I^V) + \sum_{J \neq I,M} \alpha_{IJ}'(X_J^\Phi - X_J^V)$$
⁽²⁰⁾

with the ternary interaction coefficients, α'_{IJ} , characterizing the *I*–*J* interaction in *M*, where *J* represent other solutes in the system [10].

As only the summarizing term $\Delta \overline{G}_I^E$ is correlated according to the Guttmann model and the quantities $\Delta \overline{H}_I^E$ and $\Delta \overline{S}_I^E$ itself do not explicitly appear in the thermodynamic description of interfacial segregation, we will not discuss them.

The effect of solute interaction (represented *i.e.* by α'_{IJ}) on grain boundary segregation is displayed in Figure 2. Here, the equilibrium composition is calculated for both the grain boundary of the binary *M*–*I* system in the temperature range 473–1673 K according to Equations (5) and (19) assuming a bulk concentration of $X_I^V = 0.001$ (*i.e.* 0.1 at.%), interstitial segregation of *I* at the grain boundary and the values of $\Delta H_I^{GB,0} = -30$ kJ/mol and $\Delta S_I^{GB,0} = +25$ J/(mol·K) (as for P, Sb and Sn in α -Fe). Figure 2 clearly shows the strong influence of the solute–solute interaction in the binary *M*–*I* alloy on the value of X_I^{GB} . In case of attractive interaction, $\alpha_{IM} > 0$, the grain boundary concentration of the segregant obviously is increased. Even in case of relatively low values of α_{IM} , e.g. $\alpha_{IM} = +10$ kJ/mol, the grain boundary enrichment of *I* is by tens of at.% higher than without interaction ($\alpha_{IM} = 0$). Repulsive interaction decreases the solute enrichment to a similar extent. This behavior is well understood because repulsive interaction does not allow putting another atom of the same kind in close surrounding of the atom segregated at the interface while attractive interaction exhibits an opposite effect [19]. The effect of ternary interactions (α'_{IJ} , Figure 2b) is much less pronounced as that of the binary interactions [20].

Figure 2. Temperature dependence of X_I^{GB} in (**a**) binary M–I alloy calculated according to Equations (5) and (19) using $\Delta H_I^{GB,0} = -30$ kJ/mol, $\Delta S_I^{GB,0} = +25$ J/(mol K), and various values of α_{IM} [19]; and (**b**) ternary M–I–J alloy with additionally $\Delta H_J^{GB,0} = -10$ kJ/mol, $\Delta S_J^{GB,0} = -5$ J/(mol·K) and $X_J^V = 0.03$. I_{bin} is X_I^{GB} in the binary M–I(0.1 at.%) alloy [20].



(b)

Combination of Equations (12), (15) and (19) for a binary alloy with the above condition $\Delta V_I \equiv \Delta \overline{V_I}^E$ provides us with:

$$\Delta V_{I} = \Delta \overline{V}_{I}^{E} = -\frac{X^{\Phi,sat} X_{I}^{GB}}{\frac{(X^{\Phi,sat})^{2}}{2} - \frac{\alpha_{IM}}{RT} X_{I}^{GB} (X^{\Phi,sat} - X_{I}^{GB})} \frac{d\alpha_{IM}}{dP}$$
(21)

4. Examples of Application of Thermodynamic State Functions in Interfacial Segregation

4.1. Relationship between ΔH_I^0 and ΔS_I^0 of Grain Boundary Segregation and Volume Solid Solubility

The chemical potential of the solute I at the bulk solid solubility limit, $X_I^{V,*}$:

$$\mu_I^{V,*} = \mu_I^{V,0} + RT \ln a_I^{V,*}$$
(22)

is related to the activity at the bulk solid solubility limit, $a_I^{V,*}$. We can express the Gibbs energy of segregation in an *M*–*I* system at the limit of solid solubility, ΔG_I^* , as:

$$\Delta G_I^* = \left(\mu_I^{\Phi,0} - \mu_I^{V,*}\right) - \left(\mu_M^{\Phi,0} - \mu_M^{V,*}\right) = \Delta G_I^0 - RT \ln a_I^{V,*}$$
(23)

It follows from the basic thermodynamic relationships that:

$$\Delta S_I^{V,*} = \Delta S_I^{V,0} + R \left[\frac{\partial \left(T \ln a_I^{V,*} \right)}{\partial T} \right]_{P,X_J^V}$$
(24)

Compilation of numerous literature data [21] shows that the activity of solute *I* at the solubility limit of numerous elements can be expressed by:

$$a_I^{V,*} = (X_I^{V,*})^v \tag{25}$$

as is apparent in Figure 3. In Equation (25), v is the exponent which is characteristic for the host element. For many binary systems, the product $T \ln X_I^{V,*}$ was found to be independent of temperature (Figure 4) [1,22]. It means that $\Delta S_I^{V,*} = \Delta S_I^{V,0}$ if conditions (24) and (25) are fulfilled, and:

$$\Delta H_I^* = \Delta H_I^0 - RT \ln a_I^{V,*} \tag{26}$$

i.e. [1,5]:

$$\Delta H_{I}^{0}(\Phi, X_{I}^{V,*}) = \Delta H_{CSS}^{*,(\Phi)} + vR \Big[T \ln X_{I}^{V,*}(T) \Big]$$
(27)

In Equation (27), $\Delta H_{CSS}^{*,(\Phi)}$ is the molar enthalpy of segregation of a solute with complete *volume* solid solubility in solvent *M*, and the symbol Φ characterizes a specific grain boundary [1,5]. As the product $T \ln X_I^{V,*} = const$, the above mentioned condition of temperature independence of ΔH_I^0 is preserved. Equation (27) represents an extension and a refinement of the expression $X_I^{\Phi}/X_I^V = K/X_I^{V,*}$, (K = 1.8-10.8) given by Hondros and Seah which relates the grain boundary enrichment ratio to the solid solubility limit [2], and the qualitative idea of Watanabe to extend this simple dependence to account for anisotropy of grain boundary segregation [23] and to construct the so called grain boundary segregation diagram. This idea was later experimentally proved [24]. The grain boundary segregation diagram for solute segregation in α -iron at [100] symmetrical grain boundaries is shown in Figure 5 [1,5].

Figure 3. Dependence of the activity at the volume solid solubility limit, $a_I^{V,*}$, and corresponding atomic fraction, $X_I^{V,*}$, for numerous solutes in α -iron correlated according to Equation (25) [1,21].

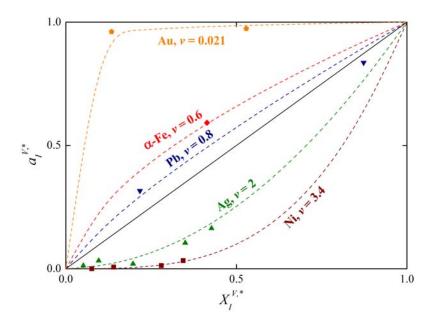
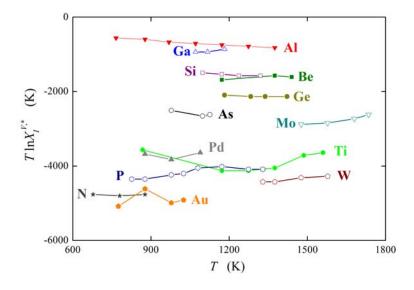


Figure 4. Temperature dependence of the product $T \ln X_I^{V,*}$ for various solutes in α -iron [1,22].



Analysis of the measured data on segregation of phosphorus, silicon and carbon at individual grain boundaries in α -iron show that the value of the exponent v = 0.77 [1,4,5] which is in good agreement with the value v = 0.6 obtained on basis of Equation (25) from data of Reference [21] (Figure 3). The value of $\Delta H_{CSS}^{*,(\Phi)}$ varies from -8 to +8 kJ/mol according to the grain boundary character (the lower value corresponds to highly segregated general grain boundaries while the latter one corresponds to the special grain boundaries characterized by low segregation levels: for a detailed explanation of this characterization see e.g. [1]).

The above mentioned measurements of grain boundary segregation in iron [1,4,5] provided us with the values of both ΔH_I^0 and ΔS_I^0 . As an example, the dependence of ΔH_I^0 and ΔS_I^0 on the misorienation

angle for [100] symmetrical grain boundaries is shown in Figure 6. It is obvious that the orientation dependences of ΔH_I^0 and ΔS_I^0 are qualitatively equivalent for all segregating elements.

Figure 5. Grain boundary segregation diagram for [100] symmetrical grain boundaries in α -iron [1,4,5]. Notice that the lines characterizing the dependence of ΔH_I^0 on $T \ln X_I^{V,*}$ are parallel for individual grain boundaries. The value of the slope in Equation (27) is v = 0.77.

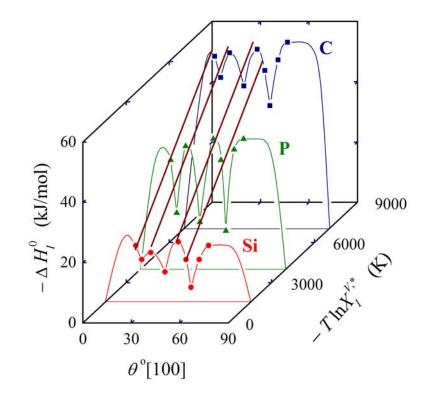
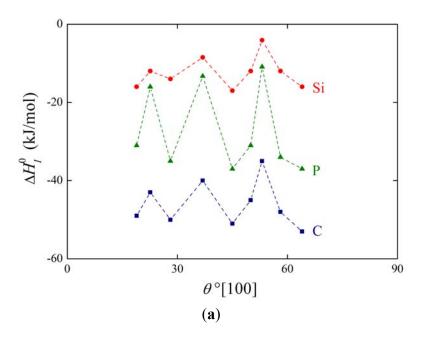
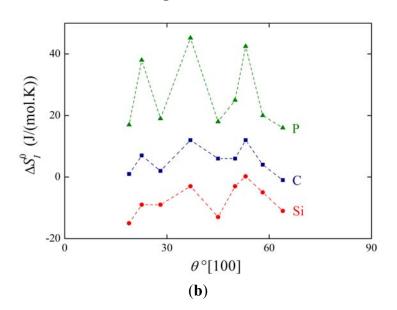


Figure 6. Anisotropy of (**a**) the standard enthalpy, ΔH_I^0 , and (**b**) the standard entropy, ΔS_I^0 , of Si, P and C segregation for [100] symmetrical grain boundaries in α -iron [1,4,5].





4.2. Compensation Effect in Grain Boundary Segregation

In principle, we can express the change of the standard molar segregation Gibbs energy of interfacial segregation, ΔG_I^0 , at constant temperature and pressure with a single intensive variable Ψ as [25]:

$$d\Delta G_I^0 = \left(\frac{\partial \Delta G_I^0}{\partial \Psi}\right)_{T,P,\Psi_I \neq \Psi} d\Psi.$$
(28)

Analogously, we can express ΔH_I^0 and ΔS_I^0 as:

$$d\Delta H_{I}^{0} = \left(\frac{\partial\Delta H_{I}^{0}}{\partial\Psi}\right)_{T,P,\Psi_{i}\neq\Psi} d\Psi, \text{ and } d\Delta S_{I}^{0} = \left(\frac{\partial\Delta S_{I}^{0}}{\partial\Psi_{j}}\right)_{T,P,\Psi_{i}\neq\Psi} d\Psi.$$
(29)

We may define a temperature T_{CE} as:

$$T_{CE} = \frac{d\Delta H_I^0}{d\Delta S_I^0} = \frac{\left(\frac{\partial\Delta H_I^0}{\partial\Psi}\right)_{T,P,\Psi_i\neq\Psi}}{\left(\frac{\partial\Delta S_I^0}{\partial\Psi}\right)_{T,P,\Psi_i\neq\Psi}} d\Psi$$
(30)

at which:

$$d\Delta G_I^0(T_{CE}) = 0.$$
⁽³¹⁾

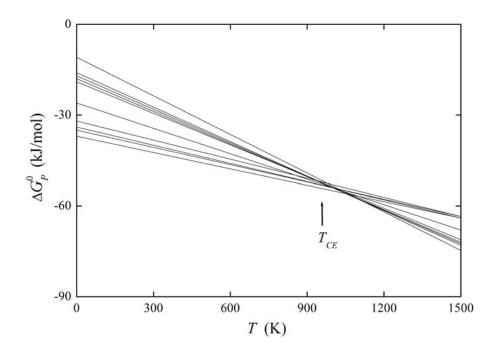
It means that the change of ΔH_I^0 with changing Ψ is *compensated* by corresponding changes of ΔS_I^0 caused by a change of Ψ . Then T_{CE} is the *compensation temperature* and the phenomenon is called *compensation effect* [1,5,26]. If we suppose that Ψ is a variable describing the structure of the grain boundary, we can read Equation (31) as providing us with the constant value of the standard Gibbs energy of a solute at any grain boundary, *i.e.*, all grain boundaries fulfilling the above conditions exhibit the same level of grain boundary segregation. If Ψ represents the nature of the solute, all grain

boundaries will exhibit the same value of the grain boundary enrichment ratio, X_I^{Φ}/X_I^{V} . The former case is documented for example on the basis of experimental data for phosphorus segregation at individual grain boundaries of α -iron in Figure 7. Let us note that condition (31) does not identify a phase transformation characterized by minimum of the Gibbs energy: phase transformation is a subcategory of the compensation effect. At T_{CE} no transformation of the boundaries occurs but they coexist besides each other, despite the temperature changes in the vicinity of T_{CE} [25,27].

Integration of Equation (30) results in [1,5]:

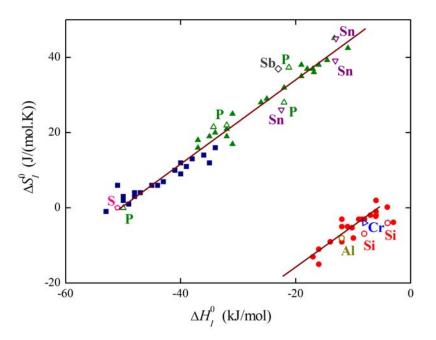
$$\Delta S_I^0(\Psi) = \Delta S^{0,CE} + \frac{\Delta H_I^0(\Psi)}{T_{CE}}.$$
(32)

Figure 7. Temperature dependence of the standard Gibbs energy of phosphorus segregation, ΔG_P^{0} , in α -iron at various [100] symmetrical grain boundaries in [1,5].



The plot of the relation between ΔH_I^0 and ΔS_I^0 for solute segregation in α -iron is shown in Figure 8. We can distinguish two branches of this dependence: they differ in the type of segregation site: the upper one corresponds to interstitial segregation ($\Delta S^{0,CE} = 56 \text{ J/(mol}\cdot\text{K})$) while the lower one to substitutional segregation ($\Delta S^{0,CE} = 5 \text{ J/(mol}\cdot\text{K})$) [1,4,5]. Individual full symbols of the same type correspond to the segregation of a solute at individual grain boundaries in α -iron, empty symbols are data found in literature (for the sources of the data, see [1,5]). Let us note that various solutes segregating at the same type of the site also fit with a single dependence (i.e. with either upper or lower branch in Figure 8). The slope of both dependences corresponds to $T_{CE} = 930$ K which suggests that the compensation temperature is characteristic for the matrix [1,5,28]. Splitting of the compensation effect into two branches confirms the fact that the compensation effect is only fulfilled if a single mechanism of the phenomenon is active. Therefore, it can be applied to otherwise independent standard quantities ΔH_I^0 and ΔS_I^0 albeit not to ΔH_I and ΔS_I which additionally change with temperature and composition.

Figure 8. Compensation effect in solute segregation at [100] symmetrical grain boundaries in α -iron [1,4,5]. Upper branch corresponds to interstitial segregation, lower branches to substitutional one.



Let us only briefly mention that Equations (27) and (32) with the above mentioned values of $\Delta H_{CSS}^{*,(\Phi)}$ and $\Delta S^{0,CE}$ can be used to predict the values of ΔH_I^0 and ΔS_I^0 of any element at any grain boundary in α -iron [1,4,5]. It is likely that such prediction may be done for other metallic solvents.

We can also express the dependence of ΔS_I^0 on the volume solid solubility. Combination of Equations (27) and (32) provides us with:

$$\Delta S_I^0(\Phi, site, X_I^{V,*}) = \left[\Delta S^{0,CE}(\Phi, site) + \frac{\Delta H_{CSS}^{*,(\Phi)}}{T_{CE}}\right] + \frac{vR}{T_{CE}} \left[T \ln X_I^{V,*}(T)\right]$$
(33)

where the notation *site* refers to the type of segregation, *i.e.*, either interstitial or substitutional. Using the mentioned data, dependence (33) is shown in Figure 9. It is clearly seen that the majority of the experimental data corresponding to both individual grain boundaries (solid symbols) and to grain boundaries in polycrystals found in the literature (empty symbols) fit fairly well to the theoretical lines of individual branches (the upper line of each branch corresponds to special boundaries while the lower one to general boundaries).

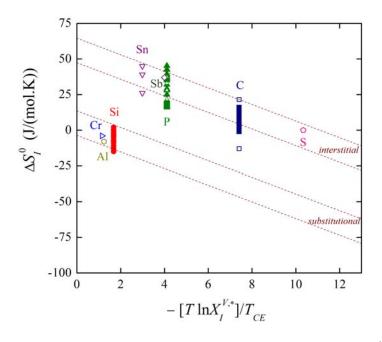
The compensation effect was observed not only in case of grain boundary and surface segregation but also for other interfacial properties, such as grain boundary migration and diffusion [5,26,27], and is present in many phenomena of physics, chemistry and biology [25].

4.3. Segregation Volume and Pressure Dependence of Grain Boundary Segregation

During time-dependent experimental studies of non-equilibrium segregation under constant stress, in the beginning a steep change of the grain boundary concentration is observed, followed by the return from an extreme value to a value almost corresponding to that measured without pressure or strain; see e.g. Figure 10 according to Reference [29]).

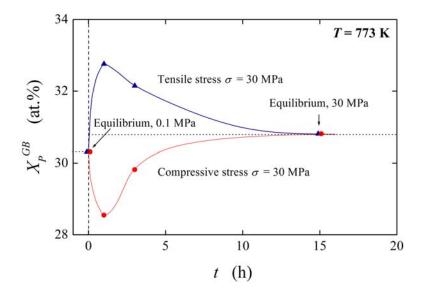
According to Equation (14) (where we use for simplicity $X^{\Phi,sat} = X^{GB,sat} = 1$, which is often applied in correlation of data on grain boundary segregation [1]), $\Delta \overline{V}_{I}^{E}$ can be obtained from experimental data [29] on pressure/stress dependence of grain boundary segregation of solutes. According to our method [30] the peak-to-peak heights in original Auger spectra were transformed into concentrations supposing simplification of the alloy to a binary Fe–P system. This procedure provides us with the values of $X_{P}^{GB} = 0.303$ representing the state under normal pressure and $X_{P}^{GB} = 0.308$ for the state in the stressed sample after equilibration (Figure 10). According to Equation (14) we obtain $\Delta \overline{V}_{P}^{E} \approx -5.1 \times 10^{-6} \text{ m}^{3}/\text{mol}$ [13]. Similar value $\Delta \overline{V}_{S}^{E} \approx -5.5 \times 10^{-6} \text{ m}^{3}/\text{mol}$ for sulphur was determined from the data of Misra [31] who studied grain boundary segregation of sulphur in a low-alloy steel (doped by 0.01 wt.% S) under plastic stress conditions at 883 K by 343 MPa. However, no changes of X_{P}^{GB} were observed after prolonged annealing of a phosphorus-doped 2.25Cr1Mo steel at 793 K under various loads [32] suggesting $\Delta \overline{V}_{P}^{E} = 0$ and thus, ideal behavior of this system.

Figure 9. Dependence of standard entropy of grain boundary segregation in α -iron on the volume solid solubility term, $(T \ln X_I^{V,*})/T_{CE}$. Solid symbols refer to segregation at individual grain boundaries [4,5], empty symbols are literature data corresponding to measurements on polycrystals [1]. The dashed lines were calculated according to Equation (33).



The value of $\Delta \overline{V}_{I}^{E}$ can also be estimated in other ways. First, $V_{Fe}^{GB} = 7.1 \times 10^{-6} \text{ m}^{3}/\text{mol}$ if pure Fe is considered instead of the 2.6NiCrMoV steel [33]. As the average boundary density is of about 50% of the bulk density [33], $V_{Fe}^{GB} = 1.42 \times 10^{-5} \text{ m}^{3}/\text{mol}$. Based on the density of FeS (4.82 g/cm³ [34]), $V_{S}^{GB} = 1.76 \times 10^{-5} \text{ m}^{3}/\text{mol}$ if GB is regarded as a Fe-48 at.%S since the atomic fraction of S in 2.6NiCrMoV is 48 at.% after stress-aging for 20 h [35]. Then $V_{S}^{GB} = 0.002 \times V_{Fe}^{GB} = 1.4 \times 10^{-9} \text{ m}^{3}/\text{mol}$, and $\Delta \overline{V}_{S}^{E} = 1.0 \times 10^{-5} \text{ m}^{3}/\text{mol}$. On the other hand, the values of $\Delta \overline{V}_{S}^{E} = -8.1 \times 10^{-6} \text{ m}^{3}/\text{mol}$, $\Delta \overline{V}_{P}^{E} = -3.0 \times 10^{-6} \text{ m}^{3}/\text{mol}$ and $\Delta \overline{V}_{Se}^{E} = -3.0 \times 10^{-6} \text{ m}^{3}/\text{mol}$ were calculated using the density functional theory technique for segregation of S, P and Se, respectively, at {012} grain boundary in Ni [36].

Figure 10. Time dependence of grain boundary segregation of phosphorus in a 0.05 wt% P-doped low alloy steel at 773 K under tensile (\blacktriangle) or compressive (•) stress of 30 MPa (according to Reference [29]).



The value of $\Delta \overline{V}_I^E$ of the order of $10^{-6}-10^{-5}$ m³/mol may seem to be low. It suggests that the pressure dependence of ΔG_I and consequently of X_I^{GB} is rather low: Even the value of $\Delta \overline{V}_I^E \approx -1 \times 10^{-5}$ m³/mol under pressure/stress of 100 MPa causes a decrease of ΔG_I by -1 kJ/mol which represents a change of X_I^{GB} in the order of several percent. This also explains why the equilibrium segregation under pressure only slightly differs from that under normal pressure [29] (see Figure 10).

Let us now consider the effect of $\Delta \overline{V}_I^E$ on X_I^{GB} in more detail. Supposing the values $\Delta H_I^0 = -30 \text{ kJ/mol}$ and $\Delta S_I^0 = +25 \text{ J/(mol} \cdot \text{K})$ (these values may represent e.g. phosphorus segregation in bcc iron [1]) and $X_I^V = 0.0001$, the grain boundary concentration of the solute under normal pressure at temperature of 800 K is $X_I^{GB}(P = 0) = 0.1554$ (*i.e.* 15.54 at.%). The pressure dependence of the calculated X_I^{GB} is plotted in Figure 11 for the values of $\Delta \overline{V}_I^E$ ranging from $-8 \times 10^{-6} \text{ m}^3/\text{mol}$ to 0. It is obvious from Figure 11 that X_I^{GB} starts to change when the pressure is higher than 10 MPa: under these higher pressures the increase of X_I^{GB} becomes quite steep. We may conclude that although the effect of elastic deformation on grain boundary segregation is small the grain boundary segregation significantly changes with increasing pressure. At high hydrostatic pressures (P > 10 GPa) this effect is rather large: In this case, the equilibrium grain boundary concentration should reach the values up to 100 at.% (*cf.* Figure 11) [13]. However, during such treatment many other processes occur in the material, e.g. dynamic recrystallization, which will influence the final segregation level; in the present modeling these effects were not taken into account.

Similarly to the basic thermodynamic state variables of segregation (ΔH_I^0 and ΔS_I^0 ; *cf.* Figure 6) we may expect that $\Delta \overline{V_I}^E$ will be anisotropic. Supposing $\Delta H_I^0 = -30$ kJ/mol, $\Delta S_I^0 = +25$ J/(mol·K) and $\Delta \overline{V_I}^E = -5 \times 10^{-6}$ m³/mol, and $\Delta H_I^0 = -10$ kJ/mol, $\Delta S_I^0 = +40$ J/(mol·K) with $\Delta \overline{V_I}^E = -2 \times 10^{-6}$ m³/mol describe segregation of *I* at general and special grain boundary, respectively, the pressure dependence of X_I^{GB} for both types of the grain boundaries at 800 K is shown in Figure 12 for $X_I^V = 0.0001$. As expected, the segregation level is lower at the special grain boundary compared to the general one. The concentration change at the special grain boundary requires higher pressure.

However, its increase may seem to be surprisingly steeper than in case of the general grain boundary. In both cases a complete saturation of the grain boundary is reached under ultimate pressures.

Figure 11. Pressure dependence of X_I^{GB} in a model M–I(0.01 at.%) alloy at 800 K for various values of $\Delta \overline{V_I}^E$ as indicated at the curves (in 10⁻⁶ m³/mol) [13].

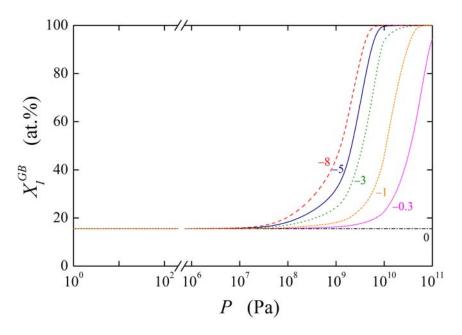
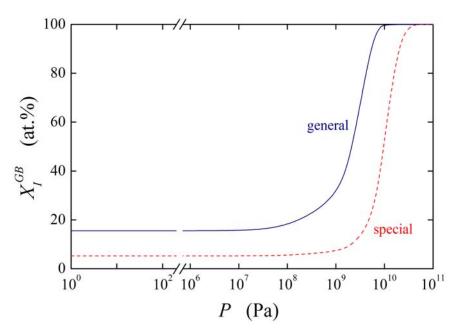


Figure 12. Pressure dependence of X_I^{GB} at special and general grain boundaries in a model M–I(0.01 at.%) alloy at 800 K. The values $\Delta H_I^{\circ} = -30 \text{ kJ/mol}$, $\Delta S_I^{\circ} = +25 \text{ J/(mol·K)}$ and $\Delta \overline{V}_I^E = -5 \times 10^{-6} \text{ m}^3/\text{mol}$ were used for general grain boundary, and $\Delta H_I^{\circ} = -10 \text{ kJ/mol}$, $\Delta S_I^{\circ} = +40 \text{ J/(mol·K)}$ and $\Delta \overline{V}_I^E = -2 \times 10^{-6} \text{ m}^3/\text{mol}$ for special grain boundary [13].



The segregation volume $\Delta \overline{V}_I^E$ depends on various intensive variables. We will document it for example of X_I^V and *T*. Differentiation of Equation (15) provides us with:

$$\left(\frac{\partial \Delta \overline{V_{I}^{E}}}{\partial X_{I}^{V}}\right)_{T,P} = \frac{RTX^{GB,sat}}{X_{I}^{GB}(X^{GB,sat} - X_{I}^{GB})} \times \left[\frac{X^{GB,sat} - 2X_{I}^{GB}}{X_{I}^{GB}(X^{GB,sat} - X_{I}^{GB})} \left(\frac{\partial X_{I}^{GB}}{\partial P}\right)_{T,X_{I}^{V}} \left(\frac{\partial X_{I}^{GB}}{\partial X_{I}^{V}}\right)_{T,P} - \left(\frac{\partial^{2} X_{I}^{GB}}{\partial P \partial X_{I}^{V}}\right)_{T}\right]$$
(34)

The first term at the right-hand side (in front of the brackets) is positive as well as the first (left) one in the brackets (supposing that less than half of the saturation limit is segregated) as X_I^{GB} increases with increasing both pressure and X_I^V . The sign of $\partial \Delta \overline{V}_I^E / \partial X_I^V$ (i.e. slope of the concentration dependence of the segregation volume) will depend on the value of the term $\partial^2 X_I^{GB} / \partial P \partial X_I^V$. Intuitively, we may expect the decrease of $\Delta \overline{V}_I^E$ (i.e. increase of its absolute value) with increasing X_I^V (and thus with increasing X_I^{GB}). For this case, $\partial^2 X_I^{GB} / \partial P \partial X_I^V$ should be positive and prevail over the first term in the brackets on the right of Equation (34). In analogy to Equation (34), the dependence of $\Delta \overline{V}_I^E$ on temperature is characterized by:

$$\left(\frac{\partial \Delta \overline{V}_{I}^{E}}{\partial T}\right)_{P,X_{I}^{V}} = \frac{RTX^{GB,sat}}{X_{I}^{GB}(X^{GB,sat} - X_{I}^{GB})} \times \left\{ \left[\frac{X^{GB,sat} - 2X_{I}^{GB}}{X_{I}^{GB}(X^{GB,sat} - X_{I}^{GB})} \left(\frac{\partial X_{I}^{GB}}{\partial T}\right)_{P,X_{I}^{V}} - \frac{1}{T}\right] \left(\frac{\partial X_{I}^{GB}}{\partial P}\right)_{T,X_{I}^{V}} - \left(\frac{\partial^{2} X_{I}^{GB}}{\partial P \partial T}\right)_{X_{I}^{V}}\right\}$$
(35)

We may expect that (negative) value of $\Delta \overline{V}_{I}^{E}$ increases with increasing temperature and reaches the value $\Delta \overline{V}_{I}^{E} = 0$ at high temperatures (e.g. close to the melting point). To bring this expectation in accordance with Equation (35), the term in the complex brackets should be positive. As $\partial X_{I}^{GB} / \partial P$ is positive and $\partial X_{I}^{GB} / \partial T$ negative (segregation decreases with increasing temperature), the term in the edge brackets on the right-hand side of Equation (35) is negative. Therefore, $\partial^{2} X_{I}^{GB} / \partial P \partial T$ on the right-hand side of Equation (35) must be negative and of higher absolute value than the other term in the complex brackets. Then $(\partial \Delta \overline{V}_{I}^{E} / \partial T)_{P,X_{I}^{V}} > 0$.

Based on Equation (21) we may demonstrate the effect of pressure on the Fowler interaction coefficient, α_{IM} (*cf.* Equation (19)), as:

$$\frac{d\alpha_{IM}}{dP} = \frac{\frac{\alpha_{IM}}{RT} X_{I}^{GB} (X^{GB,sat} - X_{I}^{GB}) - \frac{1}{2} (X^{GB,sat})^{2}}{X^{GB,sat} X_{I}^{GB}} \Delta \overline{V}_{I}^{E}.$$
(36)

Supposing $X^{GB,sat} = 1$ and $X_I^{GB} >> X_I^V$, we obtain:

$$\frac{d\alpha_{IM}}{dP} = \Delta \overline{V}_I^E \left[\frac{\alpha_{IM}}{RT} (1 - X_I^{GB}) - \frac{1}{2X_I^{GB}} \right].$$
(37)

The concentration dependences of the value of $d\alpha_{IM}/dP$ for various values of α_{IM} and $\Delta \overline{V_I}^E$ are shown in Figures 13 and 14. It is obvious that the value of the fraction on the right-hand side of Equations (36) and (37) is of the order of units in case of high grain boundary concentrations. It means that the value of $d\alpha_{IM}/dP$ is of the same order as $\Delta \overline{V_I}^E$, *i.e.* at the level of 10^{-6} m³/mol. This suggests that a change of α_{IM} by 1 kJ/mol results in an apparent change of α_{IM} with pressure or stress reaches values of the order of hundreds of MPa. The change of α_{IM} with pressure is more

pronounced for low grain boundary concentrations, however, the interaction in case of the dilute alloys can be neglected (*cf.* Equation (19)). It means that, usually, the pressure change of the interaction coefficient can be neglected.

Figure 13. Concentration dependence of $d\alpha_{IM}/dP$ for various values of α_{IM} (in units of *RT*) in a binary *M*–*I* alloy for the value of $\Delta \overline{V}_I^E = -5 \times 10^{-6} \text{ m}^3/\text{mol.}$

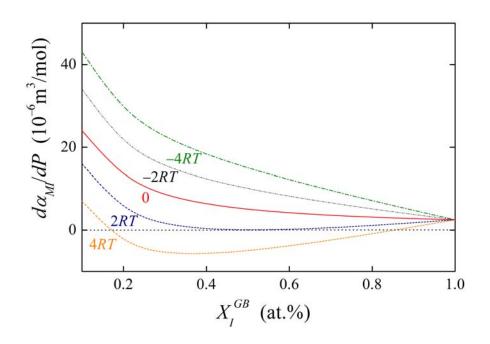
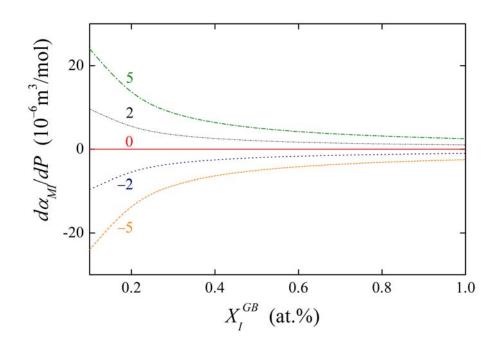


Figure 14. Concentration dependence of $d\alpha_{IM}/dP$ for various values of $\Delta \overline{V}_I^E$ in a binary *M*–*I* alloy (in 10⁻⁶ m³/mol) for $\alpha_{IM} = 2RT$.



5. Conclusions

Application of basic thermodynamics to a field of material science with important practical consequences—interfacial segregation—is presented in detail. Based on the Langmuir–McLean segregation isotherm, individual modes of thermodynamic intensive variables—which are used to describe this phenomenon—are discussed from the point of view of their physical meaning together with their potential for application. To the best of our knowledge, the segregation volume is fully defined and discussed for the first time here. It is shown that the standard molar segregation volume is zero at any temperature according to the definition of the standard states while the partial molar excess segregation is not affected by pressure in ideal systems. It is concluded that the grain boundary segregation is not affected by pressure in ideal systems whereas the real systems exhibit apparent pressure dependence. The dependences of the standard molar enthalpy of segregation on the bulk solid solubility and the enthalpy–entropy compensation effect are displayed to enable formulation of a relationship between the standard molar entropy of grain boundary segregation and the volume bulk solid solubility. In addition, a fundamental relationship is derived between the segregation excess volume and pressure changes of the grain boundary concentration of the segregation at various important consequences of the segregation volume are established.

Acknowledgments

This work was supported by the Czech Science Foundation (Projects No. GAP108/12/0144 (PL) and GAP108/12/0311 (MŠ)), by the Project CEITEC—Central European Institute of Technology (CZ.1.05/1.1.00/02.0068) from the European Regional Development Fund (MŠ), by the Academy of Sciences of the Czech Republic (Institutional Project RVO:68081723 (MŠ)), by the National Natural Science Foundation of China (Project No. 51001011 (LZ)) and by the Fundamental Research Funds for the Central Universities (Project No. FRF-TP-12-042A (LZ)).

Author Contributions

This paper was prepared in close cooperation of all four co-authors: Pavel Lejček and Siegfried Hofmann provided the main contribution to the thermodynamics of grain boundary segregation and its anisotropy including the enthalpy–entropy compensation effect. Pavel Lejček and Lei Zheng elaborated the idea of the segregation volume which was later completed by Mojmír Šob for the theoretically calculated data. Pavel Lejček wrote the draft of the article which was critically revised by all other co-authors and finalized in the agreement of all co-authors. All co-authors also approved the final version.

Conflicts of Interest

The authors declare no conflict of interest.

References

1. Lejček, P. Grain Boundary Segregation in Metals; Springer: Heidelberg, Germany, 2010.

- 2. Hondros, E.D.; Seah, M.P. Segregation to interfaces. Int. Met. Rev. 1977, 22, 262-299.
- 3. Johnson, W.C.; Blakely, J.M., Eds.; Interfacial Segregation; ASM: Metals Park, OH, USA, 1979.
- 4. Lejček, P.; Hofmann, S. Thermodynamics and structural aspects of grain boundary segregation. *Crit. Rev. Solid State Mater. Sci.* **1995**, *20*, 1–85.
- 5. Lejček, P.; Hofmann, S. Thermodynamics of grain boundary segregation and applications to anisotropy, compensation effect and prediction. *Crit. Rev. Solid State Mater. Sci.* **2008**, *33*, 133–163.
- 6. DuPlessis, J. Surface segregation. Solid State Phenom. 1990, 11, 1–125.
- Wynblatt, P.; Chatain, D. Anisotropy of segregation at grain boundaries and surfaces. *Metall. Mater. Trans.* 2006, 37, 2595–2620.
- 8. Polak, M.; Rubinovich, L. The interplay of surface segregation and atomic order in alloys. *Surf. Sci. Rep.* **2000**, *38*, 127–194.
- 9. Lewis, G.N.; Randall, M. Thermodynamics; McGraw-Hill: New York, NY, USA, 1923.
- 10. Guttmann, M.; McLean, D. Grain boundary segregation in multicomponent systems. In *Interfacial Segregation*; Johnson W.C., Blakely, J.M., Eds.; ASM: Metals Park, OH, USA, 1979; pp. 261–348.
- 11. Sutton, A.P.; Balluffi, R.W. Interfaces in Crystalline Solids; Clarendon: Oxford, UK, 1995.
- 12. Lojkowski, W. Evidence for pressure effect on impurity segregation in grain boundaries and interstitial grain boundary diffusion mechanism. *Defect Diffus. Forum* **1996**, *129–130*, 269–278.
- 13. Lejček, P.; Zheng, L.; Meng. Y. Excess volume in grain boundary segregation. J. Surf. Anal. 2014, 20, 198–201.
- Zhang, T.-Y.; Ren, H. Solute concentrations and strains in nanograined materials. *Acta Mater*. 2013, *61*, 477–493.
- 15. Erhart, H.; Grabke, H.J. Equilibrium segregation of phosphorus at grain boundaries of Fe–P, Fe–C, Fe–Cr–P, and Fe–Cr–C–P alloys. *Metal Sci.* **1981**, *15*, 401–408.
- Janovec, J.; Grman, D.; Perháčová, J.; Lejček, P.; Patscheider, J.; Ševc, P. Thermodynamics of phosphorus grain boundary segregation in polycrystalline low-alloy steels. *Surf. Interf. Anal.* 2000, *30*, 354–358.
- 17. Cottrell, A.H. Theoretical Physical Metallurgy; Edward Arnold Publ.: London, UK, 1959.
- 18. Rupp, J.; Birringer, R. Enhanced specific-heat-capacity (*c_p*) measurements (150–300 K) of nanometer-sized crystalline materials. *Phys. Rev. B* **1987**, *36*, 7888–7890.
- 19. Lejček, P. Effect of solute interaction on interfacial segregation and grain boundary embrittlement in binary alloys. *J. Mater. Sci.* **2013**, *48*, 2574–2580.
- 20. Lejček, P. Effect of ternary solute interaction on interfacial segregation and grain boundary embrittlement. J. Mater. Sci. 2013, 48, 4965–4972.
- 21. Hultgren, R.; Desai, P.; Hawkins, D.; Gleiser, M.; Kelley, K., Eds. Selected Values of the *Thermodynamic Properties of Binary Alloys*; ASM: Metals Park, OH, USA, 1973.
- Kubaschewski, O. Iron—Binary Phase Diagrams; Springer: Berlin, Germany, 1987; Massalski, T.B. Binary Alloy Phase Diagrams; ASM: Metals Park, OH, USA, 1987; Predel, B. Phase Equilibria of Binary Alloys; Springer: Berlin, Germany, 2003.
- Watanabe, T.; Kitamura, S.; Karashima, S. Grain boundary hardening and segregation in α-iron-tin alloy. *Acta Metal.* 1980, 28, 455–463.
- 24. Hofmann, S.; Lejček, P. Correlation between segregation enthalpy, solid solubility and interplanar spacing of $\Sigma = 5$ tilt grain boundaries in α -iron. *Scripta Metall. Mater.* **1991**, *25*, 2259–2262.

- 25. Lejček, P. Enthalpy–entropy compensation effect in grain boundary phenomena. Z. Metallkd. Int. J. Mater. Res. Adv. Tech. 2005, 96, 1129–1133.
- 26. Gottstein, G.; Shvindlerman, L.S. *Grain Boundary Migration in Metals*; CRC Press: Boca Raton, FL, USA, 1999.
- 27. Lejček, P. Is the compensation effect a phase transition? Solid State Phenom. 2008, 138, 339-346.
- 28. Lejček, P.; Jäger, A.; Gärtnerová, V. Reversed anisotropy of grain boundary properties and its effect on grain boundary engineering. *Acta Mater.* **2010**, *58*, 1930–1937.
- 29. Shinoda, T.; Nakamura, T. A model for the applied stress effects on the intergranular phosphorus segregation in ferrous materials. *Acta Metall.* **1981**, *29*, 1637–1644.
- Lejček, P. On the determination of surface composition in Auger electron spectroscopy. *Surf. Sci.* 1988, 202, 493–508.
- 31. Misra, R.D.K. Issues concerning the effect of applied tensile stress on intergranular segregation in a low alloy steel. *Acta Mater.* **1996**, *44*, 885–890.
- 32. Song, S.-H.; Wu, J.; Weng, L.-Q.; Liu, S.-J. Phosphorus grain boundary segregation under different applied tensile stress levels in a Cr–Mo low alloy steel. *Mater. Lett.* **2010**, *64*, 849–851.
- Jorra, E.; Franz, H.; Peisl, J.; Petry, W.; Wallner, G.; Birringer, R.; Gleiter, H.; Haubold, T. Small-angle neutron scattering from nanocrystalline Pd. *Phil. Mag. B* 1989, *60*, 159–168.
- 34. Speight, J.G. Lange's Handbook of Chemistry; McGraw-Hill: New York, USA, 2005; Table 4-1.
- 35. Xu, T.D. Grain-boundary anelastic relaxation and non-equilibrium dilution induced by compressive stress and its kinetic simulation. *Phil. Mag.* **2007**, *87*, 1581–1599.
- 36. Všianská, M.; Šob, M. Central European Institute of Technology, CEITEC MU, Masaryk University, Brno, Czech Republic. Unpublished data, 2013.

© 2014 by the authors; licensee MDPI, Basel, Switzerland. This article is an open access article distributed under the terms and conditions of the Creative Commons Attribution license (http://creativecommons.org/licenses/by/3.0/).